



## Prioritize effluent quality, operational costs or global warming? – Using predictive control of wastewater aeration for flexible management of objectives in WRRFs

**Stentoft, Peter Alexander; Munk-Nielsen, T.; Møller, Jan Kloppenborg; Madsen, Henrik; Valverde-Pérez, Borja; Mikkelsen, Peter Steen; Vezzaro, Luca**

*Published in:*  
Water Research

*Link to article, DOI:*  
[10.1016/j.watres.2021.116960](https://doi.org/10.1016/j.watres.2021.116960)

*Publication date:*  
2021

*Document Version*  
Peer reviewed version

[Link back to DTU Orbit](#)

### *Citation (APA):*

Stentoft, P. A., Munk-Nielsen, T., Møller, J. K., Madsen, H., Valverde-Pérez, B., Mikkelsen, P. S., & Vezzaro, L. (2021). Prioritize effluent quality, operational costs or global warming? – Using predictive control of wastewater aeration for flexible management of objectives in WRRFs. *Water Research*, 196, Article 116960. <https://doi.org/10.1016/j.watres.2021.116960>

---

### General rights

Copyright and moral rights for the publications made accessible in the public portal are retained by the authors and/or other copyright owners and it is a condition of accessing publications that users recognise and abide by the legal requirements associated with these rights.

- Users may download and print one copy of any publication from the public portal for the purpose of private study or research.
- You may not further distribute the material or use it for any profit-making activity or commercial gain
- You may freely distribute the URL identifying the publication in the public portal

If you believe that this document breaches copyright please contact us providing details, and we will remove access to the work immediately and investigate your claim.

1 **Prioritize Effluent Quality, Operational Costs or Global Warming? –**  
2 **Using Predictive Control of Wastewater Aeration for Flexible**  
3 **Management of Objectives in WRRFs**

4  
5 **P. A. Stentoft\*\*\*, T. Munk-Nielsen\*, J. K. Møller\*\*, H. Madsen\*\*, B. Valverde-Pérez\*\*\*, P. S.**  
6 **Mikkelsen \*\*\*, L. Vezzaro \*\*\*,\*\***

7 \* Krüger A/S, Veolia Water Technologies, Denmark (pas@kruger.dk, thm@kruger.dk, lxv@kruger.dk)

8 \*\* Department of Applied Mathematics and Computer Science, Technical University of Denmark,  
9 Denmark (past@dtu.dk, jkmo@dtu.dk, hmad@dtu.dk)

10 \*\*\* Department of Environmental Engineering, Technical University of Denmark, Denmark.  
11 (luve@env.dtu.dk, psmi@env.dtu.dk, bvape@env.dtu.dk)

12

13 **Abstract:**

14 This study presents a general model predictive control (MPC) algorithm for optimizing wastewater  
15 aeration in Water Resource Recovery Facilities (WRRF) under different management objectives. The  
16 flexibility of the MPC is demonstrated by controlling a WRRF under four management objectives,  
17 aiming at minimizing: (A) effluent concentrations, (B) electricity consumption, (C) total operations  
18 costs (sum electricity costs and discharge effluent tax) or (D) global warming potential (direct and  
19 indirect nitrous oxide emissions, and indirect from electricity production) . The MPC is tested with data  
20 from the alternating WRRF in Nørre Snede (Denmark) and from the Danish electricity grid. Results  
21 showed how the four control objectives resulted in important differences in aeration patterns and in the  
22 concentration dynamics over a day. Controls B and C showed similarities when looking at total costs,  
23 while similarities in global warming potential for controls A and D suggest that improving effluent  
24 quality also reduced greenhouse gases emissions. The MPC flexibility in handling different objectives  
25 is shown by using a combined objective function, optimizing both cost and greenhouse emissions. This  
26 shows the trade-off between the two objectives, enabling the calculation of marginal costs and thus  
27 allowing WRRF operators to carefully evaluate prioritization of management objectives. The long-term  
28 MPC performance is evaluated over 51 days covering seasonal and inter-weekly variations. On a daily

29 basis, control A was 9-30% cheaper on average compared to controls A, D and to the current rule-  
30 based control. Similarly, control D resulted on average in 35-43% lower greenhouse gasses daily  
31 emission compared to the other controls. Difference between control performance increased for days  
32 with greater inter-diurnal variations in electricity price or greenhouse emissions from electricity  
33 production, i.e. when MPC has greater possibilities for exploiting input variations. The flexibility of the  
34 proposed MPC can easily accommodate for additional control objectives, allowing WRRF operators to  
35 quickly adapt the plant operation to new management objectives and to face new performance  
36 requirements.

37

38

39 **Keywords:** Activated Sludge, N<sub>2</sub>O emissions, Nonlinear MPC, Economic MPC

40

41

## 42 **1. Introduction**

43 Automatic control strategies have been applied in Water Resource Recovery Facilities  
44 (WRRFs) for decades, mainly focusing on improving effluent quality, responding to  
45 variations in the inlet pollutant loads, and reducing chemical consumption and energy  
46 demand (Yuan et al., 2019). The latter control objective has recently gained  
47 increasing attention, as water supply and sanitation uses 2-3% of the world's electrical  
48 energy, with ranges around 1-18% in specific urban areas (Olsson, 2015).  
49 Specifically, WRRFs are not negligible, using approximately 1% of a country's total  
50 electricity consumption (Cao, 2011). This also implies a noticeable carbon footprint  
51 for urban water cycles: for example, this is estimated to be 372 kg-CO<sub>2</sub>/person/year in  
52 California, corresponding to 4% of total per capita emissions (Escriva-Bou et al.  
53 2018).

54 The diffusion of *smart grids*, favoured by the diffusion of solar and wind electricity  
55 sources, have triggered several studies which investigated the possibility of moving

56 WRRF peak consumption in time, thereby decreasing their carbon footprint. Lisk and  
57 Long (2013) and Kirchem et al. (2018) concluded that both wastewater transport and  
58 treatment can provide substantial flexibility in electricity consumption. Further  
59 investigations of the WRRF electricity consumption have identified aeration as the  
60 most demanding step, accounting for about 50% of total consumption (Longo et al.  
61 2016). Aeration control is thus essential for the plant economy, carbon footprint and  
62 for reducing peak electricity consumption.

63 Maximizing efficiency in aeration control is a task involving a trade-off of different  
64 objectives which might vary over time. Several studies have defined aeration  
65 efficiency in terms of energy usage, i.e. to minimize electricity consumption while  
66 satisfying effluent limits (Longo et al., 2020, Yuan et al., 2019). This definition  
67 assumes that lower electricity consumption would linearly lead to reductions in  
68 operational costs and/or in greenhouse gas (GHG) emissions related to the electricity  
69 production. Other studies considered effluent quality/cost by introducing weights on  
70 concentrations and electricity consumption (Yamanaka et al. 2006). However, the  
71 current development in electricity supply, going towards a higher penetration of  
72 renewable energy sources (Ren21, 2020), undermines this assumption of a direct  
73 correlation between electricity consumption and costs/emissions.

74 Using Denmark as example, the hourly electricity prices varied between -112.18  
75 DKK/MWh and 385.59 DKK/MWh on the 2019/01/14 (Nordpool, 2020), while the  
76 related GHG emissions varied between 42 kg-CO<sub>2</sub>-eq/MWh and 162 kg-CO<sub>2</sub>-  
77 eq/MWh (Energinet, 2020). This example shows how a minimal electricity  
78 consumption does not necessarily lead to minimal operational costs, since a low and  
79 constant electricity consumption would not exploit the negative price. If peak prices  
80 and emissions are distributed differently over the day, reducing GHG emissions

81 related to electricity is also different from reducing operational costs or electricity  
82 consumption.

83 An additional operational cost in Denmark is represented by the effluent tax, aiming  
84 at reducing N emissions from WRRFs, and set to 30 DKK/kg-N (Danish Ministry of  
85 Taxation, 2020). Minimizing aeration can therefore reduce N removal and thereby  
86 lead to an increase in total costs. Furthermore, controls varying oxygen conditions  
87 may promote direct GHG emissions as N<sub>2</sub>O, especially at low DO levels (Domingo  
88 Félez and Smets, 2019). This can considerably affect the carbon footprint of  
89 municipal WRRFs (Delre et al., 2019).

90 WRRF operators need flexible control strategies capable of operating at the highest  
91 level of the control hierarchy, i.e. they should be able to quickly accommodate for  
92 different management objectives (effluent quality, operational costs, electricity  
93 consumption, GHG-emissions). Model Predictive Control (MPC) fulfils these  
94 demands thanks to the possibility of using objective functions considering multiple  
95 targets. MPC uses a model of the controlled system to evaluate the effect of different  
96 control actions based on an *ad-hoc* objective function, choosing the one ensuring the  
97 best outcome. For computational reasons, MPC typically employs simple models. An  
98 advantage of MPC is that the control becomes a direct optimization problem where  
99 the design of the objective function decides the effective control. Hence, changing the  
100 objective function leads to new optima and thereby new control actions. This becomes  
101 particularly advantageous when objectives have variable inputs (see e.g. Lund et al.  
102 2018).

103 Several examples of MPC for WRRF aeration exists in literature, such as MPC based  
104 on process models (e.g. Holenda et al., 2008, Mulas et al., 2015), or black-box models  
105 using neural networks which learn from data (e.g. Foscolliano et al. 2016, Bernardelli

106 et al. 2020). However, these examples do not consider varying electricity prices or  
107 GHG emissions, and therefore they will not adapt to *smart grid* systems, characterized  
108 by price variations or by varying tariffs (as in the example from Aymerich et al.  
109 2015).

110 Varying prices can be known in advance due to the market mechanics, as in the case  
111 of the Nordpool market covering Northern Europe. If variable tariffs are present as in  
112 Spain (Aymerich et al. 2015) a price model of the tariffs can supply price variations  
113 ahead in time. If prices are uncertain but follow a certain pattern (e.g. diurnal) this can  
114 also be incorporated using a price model. Furthermore, GHG-emissions from  
115 electricity production can be forecasted using different techniques such as machine-  
116 learning (Leerbeck et al. 2020a), creating new opportunities for MPC, which can  
117 consider these future variations in the control evaluation. This approach has been  
118 tested for integrated control of pumping from sewer system basins to WRRFs  
119 (Stentoft et al. 2020a). To the knowledge of the authors, two strategies for predictive  
120 control of aeration using electricity price data are found in literature (Stentoft et al.  
121 2019a, Brok et al. 2019). However, these approaches face challenges with long  
122 optimization times (Stentoft et al. 2019a) or no direct handling of effluent limits (Brok  
123 et al. 2019). Varying GHG emissions in electricity mix have been investigated in the  
124 control of heat pumps for district heating systems (Leerbeck et al. 2020b), but not for  
125 WRRF aeration. In addition, the trade-off between operation costs and GHG-  
126 emissions will become increasingly important in case a CO<sub>2</sub> tax is introduced.  
127 However, to the authors knowledge this has not been investigated for WRRFs  
128 aeration control.

129 This paper presents a general MPC setup using stochastic differential equations which  
130 allows WRRF operators to balance between different management of objectives

131 without developing a new control strategy, i.e. by simply switching the objective  
132 function to optimize e.g. effluent, electricity consumption, aeration costs, and/or GHG  
133 emissions. The setup is tested on a small alternating WRRF (i.e. a plant where  
134 intermittent aeration allows nitrification and denitrification to occur in the same tank -  
135 Isaacs and Thornberg, 1998) in Denmark (Nørre Snede). Four objectives  
136 (minimization of effluent N levels, electricity consumption, operational costs, GHG  
137 emissions) are tested. The MPC is evaluated by analysing the changes in the aeration  
138 set-points defined by the control and the impacts on the plant daily performance and  
139 over long term. Furthermore, a combined objective function is assessed, showing how  
140 an operator can quickly modify plant operations according to different management of  
141 objectives.

142

## 143 **2. Materials and Methods**

144

### 145 **2.1 Data-driven Activated Sludge Model for nitrogen removal**

146 There are several data-driven models simulating nitrogen removal processes based on  
147 stochastic differential equations, including those developed in the 1990s (Carstensen  
148 et al. 1995) and recent developments (Stentoft et al. 2019b). Here, an adapted version  
149 of Stentoft et al. (2019b) is used. This new version introduces the state  $S_{\mu}$  which  
150 models the concentration of ammonium in wastewater arriving at the biological  
151 treatment step. In addition the model introduces the algebraic equation,  $O$ , which  
152 describes the alternating aeration signal (eq. 5). The model is derived from the  
153 ASM1s process description and it is described by the following set of equations:

$$dS_{NH} = \kappa_1(S_\mu + f(t) - S_{NH})dt - r_{Ni} \frac{O_1(t)S_{NH}}{r_{Ni}K_{NH} + S_{NH} + m_{NH}} dt + \sigma_1 d\omega_1 \quad (1)$$

$$dS_{NO} = \kappa_1(\mu_{in,NO} - S_{NO})dt + r_{Ni} \frac{O_2(t)S_{NH}}{r_{Ni}K_{NH} + S_{NH} + m_{NH}} dt - \frac{r_{Dni}(1 - O_2(t))S_{NO}}{r_{Dni}K_{NO} + S_{NO} + m_{NO}} dt + \sigma_2 d\omega_2 \quad (2)$$

$$dS_\mu = \kappa_2(\mu_{in,NH} - S_\mu)dt + \sigma_3 d\omega_3 \quad (3)$$

154 where parameters and state variables are listed in Table 1.

155

156 <Table 1>

157

158 The term  $f(t)$  provides an estimate of the diurnal variation in the incoming ammonium

159 load at the biological treatment, inspired by the harmonic formulation suggested by

160 Langergraber et al. (2008).

161

$$f(t) = \sum_{i=1}^2 cc_{2i-1} \sin\left(\frac{ipt}{p}\right) + cc_{2i} \cos\left(\frac{ipt}{p}\right) \quad (4)$$

162



163 where  $t$  is the input time [minutes],  $p$  is the period of the harmonic functions (1440  
 164 minutes for a diurnal variation), and the parameters  $cc_x$  define the shape of the  
 165 harmonic profiles.

166

167 The terms  $O_1(t)$  and  $O_2(t)$  in eq. 1-2 represent a formulation of the alternating  
 168 aeration signal with different delay for ammonium and nitrate. Here the aeration is  
 169 modelled as a sum of sigmoid-functions which allows for direct estimation of the  
 170 delay  $D_1$ ,  $D_2$  in the system. This should here be seen as a late response from when  
 171 aeration starts/stops ( $\tau_{on}/\tau_{off}$ ) to the moment when there are observable changes in  
 172 ammonium/nitrate concentrations, as also described in Stenftoft et al. (2017):

173

$$174 \quad O_j(t, \tau_{on}, \tau_{off}) = \sum_{i=0}^n \frac{1}{(1+e^{\alpha_1})^{\kappa_3} (1+e^{\alpha_2})^{-\kappa_3}} \quad (5a)$$

$$175 \quad \alpha_1 = -\kappa_4(t - \tau_{on,i} - D_j) \quad (5b)$$

$$176 \quad \alpha_2 = t - \tau_{off,i} - D_j \quad (5c)$$

177

178 In an online setting, the switching times,  $\tau_{on}/\tau_{off}$ , are determined from the control  
 179 DO set-points simply by defining  $\tau_{on}$  as the times when the DO set-point switches  
 180 from zero to a value greater than zero and vice versa (for  $\tau_{off}$ ). All the additional  
 181 parameters (listed in Table 1) are estimated automatically, without the need for  
 182 manual interventions, by minimizing a negative log likelihood function using a  
 183 gradient-based optimizer with respect to the last 24 hours of data. The setup is more  
 184 thoroughly described in Stenftoft et al. (2019b). The modelling framework specified  
 185 here (and in Stenftoft et al. 2019b) is designed to run online with parameters being re-  
 186 estimated frequently (i.e. every 6-12 hours). This implies that changes in the  
 187 biological processes or incoming water are captured when the parameters in the model

188 are updated. If changes are expected more frequently, the parameter update frequency  
189 can be increased. The uncertainty of the model (i.e. the variance/covariance matrix) is  
190 estimated using the Extended Kalman Filter (EKF) to update the model states with  
191 observations and a numerical integration scheme. This is thoroughly described in  
192 Stentoft et al. 2019.

193

## 194 **2.2 Nonlinear Model Predictive Control of Activated Sludge Processes**

195 Model Predictive Control (MPC) finds the best control action(s) based on an  
196 optimization over future objectives with respect to some objective function,  $J(u)$  with  
197 inputs  $u$ , and  $m$  constraints  $b_i$  on a constraint function  $l(u)$ . Typically this is set up as a  
198 minimization problem, and it can generally be expressed as

$$199 \min J(u) \tag{6a}$$

$$200 \text{ s. t. } l_i(u) \leq b_i, i = 1, \dots, m \tag{6b}$$

201 If either the objective function,  $J(u)$ , or the constraint function,  $l_i(u)$ , is a nonlinear  
202 function, the problem becomes a nonlinear optimization problem. This is more  
203 difficult to handle compared to a linear or convex optimization, and thereby it allows  
204 for fewer optimization variables. However, it has the major advantage that it can  
205 embrace non-linear system dynamics. The challenge in nonlinear optimization is that  
206 the objective can have several local optima, requiring good initial parameter guesses  
207 or optimization algorithms that can efficiently explore the parameter space (Lund et  
208 al. 2018). This is further elaborated for this application in Section 2.4.

209 In this MPC implementation, the goal is to find the best aeration strategy that  
210 minimizes different objectives with respect to constraints on the process and on the  
211 aeration signal itself. The aeration signal is here optimized with respect to when it

212 should be switched “on”/”off” as the DO-setpoint is set simply as a function of  
 213 ammonium concentration. Hence constraints on the aeration signal can be expressed  
 214 using simple linear constraints that govern how long aeration equipment can be “on”  
 215 and “off”:

$$216 \quad \tau_{on,i} - \tau_{off,i} \leq \tau_{max,on} \quad (7a)$$

$$217 \quad \tau_{on,i} - \tau_{off,i} \geq \tau_{min,on} \quad (7b)$$

$$218 \quad \tau_{off,i} - \tau_{on,i+1} \leq \tau_{max,off} \quad (7c)$$

$$219 \quad \tau_{off,i} - \tau_{on,i+1} \geq \tau_{min,off} \quad (7d)$$

220 Where the difference,  $\tau_{on,i} - \tau_{off,i}$ , represents the time interval when aeration is  
 221 active (“on”), and  $\tau_{off,i} - \tau_{on,i+1}$  the period when aeration is off. These time  
 222 differences have also a lower ( $\tau_{min,on}$ ,  $\tau_{min,off}$ ) and an upper ( $\tau_{max,on}$ ,  $\tau_{max,off}$ )  
 223 constraint, which are set by experienced process engineers to avoid detrimental effect  
 224 on the biological communities in the plant.

225 Biological tanks are assumed to be completely mixed reactors, i.e. effluent  
 226 concentration limits for ammonium ( $L_{NH}$ ) and total nitrogen ( $L_N$ ) can be added as  
 227 constraints:

$$228 \quad E_{24h}[S_{NH}] \leq L_{NH} \quad (8a)$$

$$229 \quad E_{24h}[S_{NO} + S_{NH}] \leq L_N \quad (8b)$$

230 where  $E_{24h}[S_x]$  are the 24-hour average effluent concentrations, which according to  
 231 the Danish legislation need to comply with effluent discharge limits. Additional  
 232 constrains can be added to comply with local discharge regulations, targeting e.g.  
 233 instantaneous discharge limits.

234

### 235 2.3 Flexible control of management objectives

236 To investigate the response of a WRRF controlled by the presented MPC, four  
237 different management objectives are investigated:

238

- 239 • *Objective A: Effluent total-N optimization*, considering only the mean effluent  
240 concentration of ammonium and nitrate.
- 241 • *Objective B: Electricity consumption optimization*, considering only aeration on-  
242 time;
- 243 • *Objective C: Total operational costs optimization*, considering electricity  
244 consumption and effluent taxes;
- 245 • *Objective D: Global Warming Potential (GWP) optimization*, considering N<sub>2</sub>O  
246 direct emissions from nitrogen removal and indirect from N discharged in the  
247 effluent, as well as indirect greenhouse gas emissions (GHG) related to electricity  
248 production;

249

250 The *optimization of effluent total-N (A)* minimizes the sum of ammonium and nitrate  
251 in the effluent over the 24-hour prediction horizon, in line with the Danish discharge  
252 regulation.

253

$$J_{(A)}(\tau_{on}, \tau_{off}) = \int_{t=0}^{24h} (S_{NH}(t) + S_{NO}(t)) dt \quad (9)$$

254

255 The *optimization of electricity consumption* (B) assumes that aeration is the most  
 256 energy-intensive step in a WRRF and does not consider variations in electricity  
 257 prices. This scenario minimizes the objective function  $J_B$ , which estimates the total  
 258 time aeration is activated during the 24-hour prediction horizon:

$$J_{(B)}(\tau_{on}, \tau_{off}) = \int_{t=0}^{24h} Air_{on}(\tau_{on}, \tau_{off}, t) dt \quad (10)$$

259 where the term  $Air_{on}(\tau_{on}, \tau_{off}, t)$  [-] is an indicator function tracking the aeration  
 260 status (set to 1 if aeration is on at time  $t$  and 0 otherwise).

261 The *optimization of total operational costs* (C) further extends objectives (A) and (B)  
 262 for areas with varying electricity prices or a tax on effluent nutrients. This scenario  
 263 minimizes the objective function  $J_C$  similar to the one used by Stentoft et al. (2019a),  
 264 which expresses the total cost in Danish Krone (DKK). This considers both the  
 265 effluent discharge tax on total-N ( $T_N$  [DKK/gN]) and the hourly electricity price (from  
 266 the day-ahead market) at the  $t$ -th hour ( $Ep_t$  [DKK/MW]) multiplied with the constant  
 267  $Ec$  [MW] which is the electricity consumption of the aeration equipment.:

$$J_{(C)}(\tau_{on}, \tau_{off}) = \int_{t=0}^{24h} (Ep_t Air_{on}(\tau_{on}, \tau_{off}, t) Ec + (S_{NH}(t) + S_{NO}(t)) T_N) dt \quad (11)$$

268

269 The *optimization of global warming potential* (D) minimizes the objective function  $J_D$   
 270 which consider the total GHG emissions as CO<sub>2</sub> equivalent [kg-CO<sub>2</sub>-eq]:

$$\begin{aligned}
J_{(D)}(\tau_{on}, \tau_{off}) = & \int_{t=0}^{24h} \left( R_{N_2O} \left( r_{NH}(t, \tau_{on}, \tau_{off}) \right) C_{N_2O, CO_2} \right. \\
& + (S_{NH}(t) + S_{NO}(t)) Eff_{N_2O} C_{N_2O, CO_2} \\
& \left. + GHG_{El,k} Air_{on}(\tau_{on}, \tau_{off}, t) \right) dt
\end{aligned} \tag{12}$$

271 where the term  $R_{N_2O}$  is the effective rate at which  $N_2O$  is created as a function of the  
272 ammonium removal rate  $r_{NH}$ . This can be estimated as the term from (1):

$$r_{NH} = r_{Ni} \frac{O_1(t, \theta) S_{NH}}{r_{Ni} K_{NH} + S_{NH} + m_{NH}} dt \tag{13}$$

273 This objective function thus considers  $N_2O$  production as a function of ammonia  
274 removal rate, modelled according to two correlations found in Blum et al. (2018).  
275 This model considers  $N_2O$  emissions by nitrifying nitrification pathway, which is  
276 dominant in several plant configurations working with ammonia based aeration  
277 control when nitrification capacity is limited (e.g., winter time; Ahn et al., 2010, Porro  
278 et al., 2017, Bellandi et al., 2020). In addition, indirect  $N_2O$  emissions due to nitrogen  
279 discharged in the effluent are estimated as a fraction of effluent total nitrogen ( $Eff_{N_2O}$ )  
280 that is calculated based on IPCC guidelines (Bartram et al., 2019). Indirect GHG  
281 emissions from electricity production in the Danish market ( $GHG_{El,k}$ ) are calculated  
282 based on data from Danish electricity network operator, presented in section 2.5  
283 (Energinet, 2020).

284

285 To illustrate how the MPC can combine different management objectives, a combined  
286 objective function  $J_{(C,D)}(\tau_{on}, \tau_{off})$  is used, where a weight  $\alpha$  [-] is used to prioritize  
287 among the different objectives:

$$J_{(C,D)}(\tau_{on}, \tau_{off}) = \alpha J_{(D)}(\tau_{on}, \tau_{off}) + (1 - \alpha) J_{(C)}(\tau_{on}, \tau_{off}) \quad (14)$$

288 Where  $\alpha$  ranges between 0, giving full priority to costs minimization, and 1, giving  
 289 full priority to minimizing GHG emissions.

290

#### 291 **2.4 Simplifications for implementation in an online setup**

292 All the considered objective functions are non-linear. Since the number of switching  
 293 times (i.e. the controlled variables which govern when aeration is switched on and  
 294 off) increase with the length of horizon, the optimization can become difficult for long  
 295 horizons (i.e. the period ahead in time which the MPC strategy optimizes). Hence,  
 296 simplifications are needed to speed up the calculation time and to reduce the number  
 297 of parameters to be estimated, thereby enabling the application of the proposed MPC  
 298 in an online setup.

299

300 Here a prediction horizon of 24 hours is considered as the legislation requirements  
 301 consider 24 hour average effluent concentrations. The calculations of the constraints  
 302 on the 24 hour effluent concentrations (eq. 8a,b) are implemented by adding two state  
 303 variables to those listed in eq. 1-3: average ammonium,  $S_{\mu,24h,NH}$ , and average total-  
 304 N,  $S_{\mu,24h,N}$ .

$$305 \quad S_{\mu,24h,NH} = \frac{\int_{t=0}^{24h} S_{NH} dt}{24h} \quad (15a)$$

$$306 \quad S_{\mu,24h,N} = S_{\mu,24h,NH} + \frac{\int_{t=0}^{24h} S_{NO} dt}{24h} \quad (15b)$$

307 These new states can be seen as mean concentration over time as the integral sums the  
308 concentrations over the 24 hr horizon.

309 In case of very low discharge limits or extraordinarily high incoming nutrient loads,  
310 the MPC might fail to satisfy the constraints on the effluent 24h average concentration  
311 (eq. 8a,b). Nevertheless, the optimizer should still be capable of providing an  
312 acceptable solution with respect to eq. 8, disregarding the objective function  $J$ . From a  
313 MPC point of view, this implies that eq. 8 should be implemented as soft constraints  
314 i.e., as an expression added directly in the objective function. Hence two additional  
315 terms are added to the functions  $J_{A-D}$ .

$$P_{NH} = \frac{ze^{S_{\mu,24h,NH}}}{1 + e^{-100(S_{\mu,24h,NH} - L_{NH})}} \quad (16a)$$

$$P_N = \frac{ze^{S_{\mu,24h,N}}}{1 + e^{-100(S_{\mu,24h,N} - L_N)}} \quad (16b)$$

316 Where the constant  $z$  is a sufficiently large number which secures that the penalties  
317  $P_{NH}$  and  $P_N$  are prioritized over other terms in the objective function when the means  
318  $S_{\mu,24h,NH}$  and  $S_{\mu,24h,N}$  are larger than the limits  $L_{NH}$  and  $L_N$  respectively.  
319

320 The number of parameters to optimize is reduced by parameterizing the vectors of  
321 switching times,  $\tau_{on} / \tau_{off}$ . Here the parameterization of  $\tau_{on,i} / \tau_{off,i}$  also includes the  
322 constraints on the aeration equipment (eq. 7) and new input vectors,  $k_{on} / k_{off}$  which  
323 consist of real numbers (and fewer control variables as compared to optimizing  
324 directly on the switching times,  $\tau_{on} / \tau_{off}$ ).

325



$$\begin{aligned} \tau_{on,i}(k_{on}, \tau_{max,on}, \tau_{min,on}, \tau_{on,i-1}) & \quad (17a) \\ & = \tau_{on,i-1} + \tau_{min,on} + \frac{\tau_{max,on} - \tau_{min,on}}{1 + e^{Sp(k_{on})}} \end{aligned}$$

$$\begin{aligned} \tau_{off,i}(k_{off}, \tau_{max,off}, \tau_{min,off}, \tau_{off,i-1}) & \quad (17b) \\ & = \tau_{off,i-1} + \tau_{min,off} + \frac{\tau_{max,off} - \tau_{min,off}}{1 + e^{Sp(k_{off})}} \end{aligned}$$

326

327 The function  $sp(\cdot)$  is a periodic spline function with coefficients described by the  
 328 input vectors  $k_{on}$  and  $k_{off}$ . This implementation allows choosing how many splines  
 329 and thus how many parameters,  $k_{on}$ ,  $k_{off}$ , are needed for the optimization.  
 330 Generally, a greater number of parameters allows for a more detailed optimization of  
 331 the controlled process, but results in a greater number of local minima, thus becoming  
 332 more difficult to optimize. Here a total of 12 parameters are found to be sufficient  
 333 considering the dynamics and inputs.

334

335 The relatively low number of optimization variables, combined with the fast  
 336 evaluation of the objective function, allows for the use of global optimization  
 337 algorithms to minimize the objective function. In this study, the Shuffled Complex  
 338 Evolution (SCE) algorithm (Duan et al., 1993) is used. SCE is run with a maximum of  
 339 5000 function evaluations, taking approximately 60 seconds to run on a normal PC  
 340 (CPU is an Intel Core i7-6600 with 2.60 GHz), and, generally, ensuring convergence  
 341 to the global optimum. This is considered sufficient, as decisions should, not be made  
 342 more often than every 20 minutes. The model and optimization algorithm are  
 343 implemented in R and C++, using the TMB package for R (Kristensen et al. 2016).

344 This package compiles the model written in C<sup>++</sup> and supplies the objective function as  
345 an R-object for easy use with various optimization algorithms.

346

## 347 **2.5 Case study**

348 The presented MPC setup is tested by using data from the Nørre Snede WRRF  
349 (Denmark). This is a small plant with a biological treatment volume of 3500m<sup>3</sup> and an  
350 average daily inlet volume of 1.350m<sup>3</sup> (in dry weather), yielding a hydraulic retention  
351 time of 2.6 days. The biological reactor is bottom aerated. Air diffusers are operated  
352 with alternating control, which implies that water is aerated in cycles to shift between  
353 aerobic and anoxic conditions (referred to as “on” and “off” control or intermittent  
354 aeration). Intermittent aeration at Nørre Snede WRRF is currently controlled using an  
355 advanced Rule-Based Control (RBC) strategy, which switches aeration on and off as a  
356 function of online ammonium and nitrate measurements taken every 5 minutes (Isaacs  
357 and Thornberg, 1998). Additionally, DO set-point is controlled as a function of the  
358 latest ammonia measurement every 2 minutes, following a cascade control structure  
359 (larger ammonia concentrations results in higher DO set-points – cf. Isaacs and  
360 Thornberg, 1998). The main scope for this control is simultaneous carbon and nutrient  
361 removal, as phosphorus is removed using chemical precipitation. However, carbon is  
362 not monitored at Nørre Snede WRRF, as WRRF designed for nitrogen removal  
363 demand large SRTs which sustain effective carbon removal. The plant is further  
364 described in Stentoft et al. (2019b).

365 Volatile suspended solids are assumed to be 3g-VSS/L, typical for activated sludge  
366 systems (Tchobanoglous et al. 2004). The different constants related to the objectives  
367 listed in section 2.3 are summarized for Nørre Snede WRRF in Table 1.

368

369 <Table 2>

370

371 Hourly electricity prices ( $Ep_t$ ) for the Denmark West market were retrieved from the  
372 public online databases of the European power exchange Nord Pool (Nordpool,  
373 2020). Similarly, 5-minute GHG emissions from electricity production ( $GHG_{EL,k}$ )  
374 were retrieved from public databases of the Danish electricity grid operator  
375 (Energinet, 2020).

376

377 Figure 1 shows daily prices and GHG emissions for 51 days in the period from  
378 2019/01/14 to 2020/02/18, highlighting both inter- and intra-daily variations. The first  
379 day (2019/01/14) is chosen as an example to illustrate the MPC response to daily  
380 variation. The subsequent 51 days are chosen at an 8-day interval in order to obtain a  
381 dataset that is equally distributed among different weekdays and covers all year  
382 seasons.

383

384 <Figure 1>

385

386

## 387 **2.6 MPC Evaluation**

388 The performance and verification of the presented MPC is investigated by looking at  
389 different aspects using the MPC model described in section 2.1 and the specifications  
390 of constraints and control in section 2.2-2.4.

391

392 *WRRF daily performance under different management objectives*

393 To qualitatively verify the MPC implementation and to compare the effects on the  
394 WRRF performance of the four management objectives listed in section 2.3, a first  
395 analysis is performed on aggregated daily values, followed by a comparison of the  
396 plant outlet over the 24-hr period covering the example day (2019/01/14). The plant  
397 performance is evaluated using different performance indicators, reflecting the  
398 different management objectives, and compared against the existing control (RBC):

- 399 • Effluent quality, expressed by  $\text{NH}_4$ ,  $\text{NO}_3$  and total-N effluent concentrations,  
400 to evaluate performance in nutrient removal;
- 401 • Operational costs, calculated as total costs, electricity costs and effluent  
402 taxation costs, to evaluate financial performance;
- 403 • Efficiency indicators, expressed by relative aeration on-time, average  
404 electricity consumption and average electricity GWP emissions. This is to  
405 evaluate the control prioritizes with respect to the inputs
- 406 • GWP indicators, expressed as total GHG emissions,  $\text{N}_2\text{O}$ -emissions and  
407 indirect GHG emissions, from electricity consumption, to evaluate climate  
408 performance.

409 The MPC evaluation uses the model parameters listed in Table 1, and the electricity  
410 prices and GHG emissions highlighted in Figure 1.

411 The MPC response to dynamics in electricity costs and GHG emissions is investigated  
412 by looking at the cumulative functions of total costs and GHG emissions over the  
413 optimization horizon.

414

#### 415 *MPC response to varying effluent limits*

416 To verify the correct implementation of soft constrains and to evaluate the MPC  
417 response to different discharge limits, 30 different optimizations are run for each

418 management objective by increasing the limit  $L_{NH}$  in steps of 0.05 from 0.5 to 2  
419 mgN/L.

420

#### 421 *Multiple objectives and marginal costs*

422 To verify eq. 14, The function and trade-off are evaluated by using a sequence of  
423 values for  $\alpha$ , ranging from 0 to 1. Furthermore, this objective function makes it  
424 possible to investigate the marginal costs of preferring GWP compared to total costs.

425

#### 426 *Long term performance evaluation*

427 The proposed MPC is used to control WRRF operation over the 51 days shown in  
428 Figure 1: given four different objectives, this yields to 204 optimizations in total.  
429 Potential correlations between intra-diurnal differences in costs,  $id_{cost}$ , and GHG  
430 emissions,  $id_{GHG}$ , in the optimized objective function values are investigated using  
431 these 204 optimizations.

432

$$id_{cost} = J_{(B)} - J_{(C)} \quad (18a)$$

$$id_{GWP} = J_{(A)} - J_{(D)} \quad (18b)$$

433

### 434 **3. RESULTS AND DISCUSSION**

435

#### 436 **3.1 Model implementation**

437 The estimated model parameters from Nørre Snede WRRF for the example day are  
438 listed in Table 1 with a description. An example of model fit with a 3 hour prediction  
439 is shown in Figure 2.

440

441 <Figure 2>

442

443 Figure 2 shows how the model captures the dynamics of the alternating control as the  
444 concentrations increase/decrease as expected when aeration is turned on/off. In  
445 addition, the uncertainty of the model seems reasonable as it increases with the  
446 prediction horizon, which during the estimation period is only until next available  
447 observation. This model is used in the following as basis for the predictive control.

448

449

### 450 **3.2 WRRF daily performance under different management objectives**

451 Figure 3 shows the optimal control obtained in the four management objectives for  
452 the example day (Figure 1).

453

454 <Figure 3>

455 <Table 3>

456

457 The dynamics seen in Figure 3 and the WRRF performance indicators for the whole  
458 day (Table 3) highlight some interesting findings.

459

#### 460 *Effluent quality*

461 The differences in the concentration values and dynamics under the different  
462 optimization objectives are clearly shown. All objectives comply with the soft  
463 constraints in (eq. 16). The greatest difference is noted when using function  $J_{(C)}$   
464 (Figure 3a), which has longer aeration phases and short non-aerated intervals in the

465 early morning and minimizes aeration in the afternoon. This is a direct response to the  
466 negative electricity prices between 00:00 and 05:00 (Figure 1a), which are exploited  
467 by the MPC. The effluent concentrations under objective A and D show similar  
468 patterns, but ammonium concentrations are slightly higher in objective D, meaning  
469 that less aeration is used. This is the consequence of the minimization of carbon  
470 footprint derived from energy used for aeration. The ammonium concentrations are  
471 generally increased for objective B, where electricity is minimized. Here ammonium  
472 is kept as high as possible within constraints (1.5 mg-N/l).

473

#### 474 *Operational costs*

475 The average price of consumed electricity (i.e. the price when electricity is used) is  
476 approximately 30% lower for objective C compared to the others (Table 3; 174.2 vs  
477 247.5, 245.7, 248.0 and 259.8 DKK/MWh), while smaller differences are observed  
478 among the other objectives. The electricity cost for RBC is slightly higher, due to a  
479 long non-aerated phase during the negative price period. The lowest electricity cost is  
480 (C), even though it uses more electricity compared to both (B) and the RBC. The  
481 difference in electricity costs of (A), (B), (D) and the RBC are characterized by their  
482 differences in relative amount of aeration.

483 The low average electricity price is also the reason why objective C leads to 13.9%  
484 lower total costs (Table 3; 247.7 DKK vs 279.4 DKK), even though it requires 6.2%  
485 more aeration compared to objective B (39.5% vs 33.3% aeration time). It should  
486 also be noted that optimizing costs and electricity consumption are, respectively,  
487 19.5% and 9.2% cheaper than the current RBC (which uses 324.2 DKK). This is  
488 because of a combination of lower electricity prices (for C), and a better balance

489 between taxes and electricity consumption achieved by approaching to discharge  
490 limits (for B and C).

491

492 *GWP*

493 The average GWP from electricity consumption for (D) is similar to the other  
494 strategies indicating that this factor does not necessarily affect the optimal control  
495 actions (Table 3; 112.6, 114.0, 102.7, 113.1 and 115.6 kg-CO<sub>2</sub>-eq/MWh for A-D and  
496 RBC respectively) . However, N<sub>2</sub>O emissions are 3-4 times larger in , B, C and the  
497 RBC compared to A and D (Table 3; 69.2, 282.4, 227.9, 64.7 and 219.6 kg-CO<sub>2</sub>-eq  
498 for A-D and RBC respectively). This corresponds to a reduction in GWP of 50.3%,  
499 42.8% and 42.4% lower in Objective D compared to B, C and the RBC, respectively.

500 This indicates that optimizing for low effluent nitrogen concentration is closer to  
501 minimizing GHG emissions and hence plants operated with this management  
502 objective might already have lower GWP than plants focusing on other objectives.

503 Comparing Objective C against B results in a 13.1% lower GWP, suggesting that  
504 Objective C, despite higher electricity consumption, is better in terms of both costs  
505 and GWP compared to minimization of electricity consumption. This difference is  
506 explained by the difference in N<sub>2</sub>O emissions, which is investigated further in the next  
507 section. Finally, it should be noted that Objective D, optimizing GWP, costs 30.9 %  
508 more compared to Objective C, indicating that a trade-off between operational costs  
509 and GWP needs to be made by WRRF operators. This picture may change if a CO<sub>2</sub>  
510 tax on WRRF GHG-emissions is imposed.

511

512 **3.3 Objective function dynamics**



513 Figure 4 shows the dynamics of the different strategies in terms of cumulated  
514 electricity costs and N<sub>2</sub>O emissions over the simulated example day.

515

516 <Figure 4>

517

518 Figure 4 illustrates how the MPC in C exploits better the negative prices, as after the  
519 first 8 hours the cumulative cost is still negative. Furthermore the slope on the  
520 cumulative curve is less steep compared those of Objectives A and D, resulting in an  
521 overall cost reduction. Because of the heavy aeration in the first 10 hours (where  
522 electricity prices were low), Objective C also manages to keep ammonium  
523 concentrations and therefore it keeps removal rates, sufficiently low to avoid large  
524 N<sub>2</sub>O emissions during this period. However, Objective D manages to achieve low  
525 N<sub>2</sub>O emission over the entire horizon by balancing ammonium concentration at a  
526 sufficiently low level which keeps the ammonium removal rates (eq. 13) low.

527

### 528 **3.4 MPC response to varying effluent limits**

529 The total costs and global warming potential that is found when optimizing the same  
530 scenario as in Figure 3 is investigated. Here the effluent ammonium limits is changed,  
531 and the result is shown in Figure 5.

532

533 <Figure 5>

534

535 At low effluent requirements (i.e. ammonium <0.8 mgN/L) MPC perform similarly  
536 for all objectives. This is because the main MPC goal becomes to satisfy effluent limit  
537 in all cases. When the effluent limit is increased, it becomes possible for the MPC to

538 prioritize aeration in different periods and hence different outcomes between  
539 objectives are observed. This verifies the effect of the soft-constraint, which  
540 dominates the MPC decisions when discharge requirements are not satisfied.

541 The total operational costs are reduced in all cases until A and D stabilize around 1.25  
542 mg-N/L. This suggests that the effluent requirements are not important for A and D,  
543 which already tend to minimize effluent nitrogen emissions. In the case of B and C,  
544 total costs are further reduced, and it is likely that for C the cost would decrease  
545 further, albeit little, if the limit was increased more than 2 mg-N/L. Surprisingly, the  
546 cost of Objective B starts to increase at some point, and thereby the difference  
547 between Objective C and B increases above approximately 1.5 mg-N/L. This is  
548 because the contribution of the effluent tax to the total costs overcomes the additional  
549 savings in electricity consumption.

550 For GWP, Objective A and D stabilize above 1.25 mg-N/L, suggesting that, as for  
551 total costs, effluent requirements become unimportant for MPC. Objective B and C  
552 increase GWP until roughly 1.4 mg-N/L, after which they decrease slowly. The initial  
553 increase is caused by the higher N<sub>2</sub>O-emissions as consequence of the lower aeration,  
554 which results in higher ammonium removal rates (aeration time is reduced, and thus  
555 ammonia oxidation rates increase due to ammonia accumulation). The later decrease  
556 in GWP is caused by the fact that the frequency and duration of aeration is so low that  
557 the effective aeration time and thus total emissions are reduced, even though the  
558 emission rate is high during aeration.

559 This highlights that with the management objectives from B or C, lower discharge  
560 limits do not necessarily lead to better performance in terms of GWP. Furthermore it  
561 highlights that indirect N<sub>2</sub>O emissions related to total-N in the effluent are  
562 comparably much lower than direct emissions from the WRRF.

563

### 564 **3.5 Multiple objectives and Marginal Costs**

565 Figure 6 compares the operational costs and GWP for the optimization performed by  
566 using the combined objective function (eq. 18), showing the trade-off between the two  
567 management objectives.

568

569 <Figure 6>

570

571 For example, a reduction of GWP by 125 kg-CO<sub>2</sub>-eq (42%) results in an increase in  
572 costs of about 50 DKK (20%), corresponding to a marginal cost of 0.4 DKK/kg-CO<sub>2</sub>-  
573 eq. This is obtained with a weight  $\alpha$  around 0.65 (i.e. MPC puts a 65% weight on  
574 GWP and 35% on costs). Figure 6 shows how the trade-off does not follow a linear  
575 trend, highlighting how optimization of GWP and total costs require different control  
576 actions. Therefore, the marginal cost depends on the chosen weight, and the definition  
577 of  $\alpha$  thus requires a careful analysis. For instance, high prioritization of GWP ( $\alpha > 0.8$ )  
578 does not lead to important reduction of GWP, but it increases costs from roughly 300  
579 to 335 DKK. Arguably WRRF managers should define a weight that balances GHG  
580 emission (especially N<sub>2</sub>O emission rates) while still leaving the MPC flexibility to  
581 exploit the opportunities offered by low electricity prices. In addition, it is noted that  
582  $\alpha$  values ranging from 0.2 to 0.75 will lead to a control strategy which in this case  
583 performs better than the current RBC on both total costs and GWP.

584

### 585 **3.6 Long term performance**

586 Figure 7 shows a summary of the results for the four optimization objectives  
587 performed over the 51 days shown in Figure 1 in terms of operational costs and GWP  
588 indicators.

589

590 <Figure 7>

591 <Figure 8>

592

593 Clearly, better performance is obtained for indicators specifically targeted by the  
594 optimization objective. Objective B and C, focusing on reduction of operational costs  
595 and electricity, show average costs that are not significantly different (using a 95%  
596 confidence level), with only a 3.4% difference (it is though noted that the difference is  
597 significantly larger than zero). However, when looking at single days (Figure 8a),  
598 differences appear between the two objectives for days with high inter-diurnal  
599 variations, while the difference is relatively small for most of the simulated days. It is  
600 difficult to conclude whether the relationship is linear or exponential, but it can be  
601 observed that the variance also increases with increasing inter-diurnal variations. This  
602 trend is interesting when considering that future electricity prices might show even  
603 greater inter-diurnal variations due to increasing amounts of renewables (REN21,  
604 2020) and/or implementation of varying CO<sub>2</sub>-dependent taxes/tariffs.

605 Compared to the other objectives, optimizing total costs is significantly cheaper  
606 compared to A, D and the baseline RBC, with 29.6%, 19.2% and 9.2% lower costs,  
607 respectively. Surprisingly, Objective A, C and D obtain the three lowest minimum  
608 costs (leaving out B), as indicated by the bottom of the whiskers in Figure 7(a). These  
609 values are all found in a day with 12 hours of negative prices (2019/12/16) when A

610 and D, which prioritize to higher aeration, “earns” money during half of the day while  
611 still reducing the effluent tax.

612

613 The GWP is reduced when directly targeted by the objective function (Objective D)  
614 or when minimizing N in the effluent (Objective A). D has a mean GWP 42.5%,  
615 40.9% and 34.9% lower than B, C and RBC, respectively. When compared to  
616 Objective A, the mean is not significantly lower (13.9%) due to the relatively large  
617 variances (but, the difference is significantly larger than zero). As for total costs,  
618 significant differences between Objective A and D appear when looking at individual  
619 days (Figure 8b), with greater divergences in days with greater inter-diurnal variations  
620 in GHG emissions from electricity production. However, the trend has a larger  
621 variance compared to the one observed for costs, due to the contribution of N<sub>2</sub>O  
622 emissions, which are independent from the electricity source. In both cases, part of the  
623 variation can also be explained by the fact that the distribution of highs and lows  
624 within the electricity- price/GHG series are important for the actual potential for  
625 exploitation. Hence some days are simply easier to distribute aeration in “smart” ways  
626 than others.

627 The minimum GWP obtained in Objective C is relatively lower compared to those  
628 obtained for B and RBC. This is because the low price periods which are exploited by  
629 A have the added benefit that ammonium removal rates become smaller, hence less  
630 N<sub>2</sub>O is created (as also observed for the example day in Figure 4b). Furthermore, low  
631 price periods typically correspond to lower indirect GHG emissions, thanks to the  
632 Danish electricity mix. The high extreme value obtained for Objective A (the whisker  
633 in Figure 7b) is caused by a day with very high electricity GHG-emissions  
634 (2019/05/21, ranging from 259 – 439 kg-CO<sub>2</sub>-eq/MWh).

635

### 636 **3.7 Future Outlook**

637 The proposed management objectives can be expanded to enhance the plant  
638 performance both in terms of total operational costs and GWP. For example, total  
639 costs can be further reduced by including other electricity markets in the objective  
640 function. While in this study only the “day-ahead market” is considered, the balancing  
641 market (demand-response) seems to be particularly interesting for wastewater  
642 treatment (Brok et al., 2019). This expansion would require a stochastic MPC strategy  
643 where both upregulation (use less electricity on a short notice) and downregulation  
644 (use more electricity on a short notice) are built into the objective function. Variable  
645 tariffs which are present in some areas in order to promote peak shaping should also  
646 be investigated (Aymerich et al. 2015). Thus, it is noted that the generality of the cost  
647 function allows for adding this when creating the future price input. The Danish  
648 legislation also taxes phosphorus and organic carbon emissions, creating the  
649 possibility for further extension of the objective function. Including these substances  
650 would require an additional model using stochastic differential equations (Lindstrøm  
651 et al., 2019) which, ideally, should also include predictive control of chemical dosing.  
652 Currently the DO setpoint when aeration is “on” is not considered in the MPC.  
653 Instead it is set by the plant (in this case as a function of ammonia concentrations).  
654 However, to refine the strategy, the specific DO setpoints (and not just the switching  
655 times) would be beneficial to include directly in the optimization.

656

657 The calculation of N<sub>2</sub>O is based on empirical findings on laboratory scale partial  
658 nitritation Anammox reactor, where emissions were driven by nitrifying nitrification  
659 pathway (Blum et al., 2018a). We note, however, that heterotrophic and nitrifying

660 denitrification pathways may also contribute to the overall emissions (Chen et al.,  
661 2019) and should be considered for more reliable optimization. There is relatively  
662 extensive literature on different statistical models relating different operational  
663 parameters and nitrous oxide emissions, which could be applied for the objective  
664 function (Vasilaki et al., 2018, Bellandi et al., 2020). Furthermore, these correlations  
665 could be re-calibrated with soluble N<sub>2</sub>O online data (where available). Additionally,  
666 several studies have suggested different ratios and more detailed models, accounting  
667 for all pathways contributing to N<sub>2</sub>O emissions from activated sludge processes  
668 (Domingo Félez and Smets, 2016). This shows how the prediction of N<sub>2</sub>O emissions  
669 is affected by a large level of uncertainty, which can be overcome by including N<sub>2</sub>O  
670 as a state in the system of coupled stochastic differential equations. This new state  
671 should ideally be calibrated with online N<sub>2</sub>O measurements to accommodate changes  
672 in plant due to seasonality (i.e., temperature), solid retention time, dissolved oxygen,  
673 pH or other crucial parameters (Blum et al., 2018b; Daelman et al., 2015; Massara et  
674 al., 2017; Noda et al., 2004). In addition, objective functions that also consider the  
675 hydraulic capacity of plants, including secondary clarifiers and return sludge, could be  
676 designed. This would be particularly useful for handling increased inlet flow during  
677 wet-weather events.

678 Finally, it is necessary to further validate the MPC framework, as the simple model  
679 used for optimizing and evaluating control performance does not include all the  
680 biological processes relevant in a WRRF. Further studies are thus suggested for (i)  
681 evaluating the MPC using detailed biological models (Henze et al., 2000) both for the  
682 tested configuration (alternating plant) and in benchmark setup (Jeppsson et al.,  
683 2007); and (ii) full scale testing of the long-term performance of the proposed control  
684 strategy.

#### 685 **4. Conclusion**

686 A flexible model predictive control (MPC) framework for optimizing aeration in  
687 WRRF was presented, allowing WRRF operators to optimize plant controls according  
688 to different management objectives over a 24 hour prediction horizon. The framework  
689 was tested with data from the Danish electricity grid and the Nørre Snede WRRF.  
690 Four different objective functions were investigated and evaluated with an objective  
691 analysis using different data inputs. The four objectives minimize total operational  
692 costs, electricity consumption, global warming potential (GWP), and effluent total-N.  
693 The study revealed how the four controls resulted in quite different in terms of the  
694 resulting aeration patterns, and hence dynamics of ammonium/nitrate concentrations  
695 in the biology tanks and in the effluent.

696 Controls optimizing total costs and electricity consumption both prioritized to aerate  
697 less. Controls focusing on effluent quality and GWP both resulted in lower effluent  
698 concentrations, showing how a management objective optimizing effluent quality can  
699 also be optimizing GWP.

700 The trade-off between costs and GWP was evaluated using a combined objective  
701 function. This analysis revealed that the marginal costs of an example day when  
702 prioritizing GWP over costs was ~0.4 DKK/kg-CO<sub>2</sub>-eq.

703 MPC performance was investigated over 51 days, showing how the control  
704 optimizing costs was 19.2%, 29.6% and 9.2% cheaper compared to controls  
705 optimizing for GWP, effluent N-concentrations, or the currently implemented rule  
706 based control strategy (RBC). Similarly, the control optimizing GWP resulted in  
707 40.9%, 42.5%, 13.9% and 34.9% lower emissions than the other controls optimizing  
708 for costs, electricity consumption, effluent quality, and RBC respectively.



709 Comparison between objectives revealed a correlation between inter-diurnal  
710 difference in prices/GHG-emissions and the potential savings, where larger difference  
711 generally led to larger savings. This indicates that the current potentials might  
712 increase in a future energy objective with more fluctuating energy sources. Finally, it  
713 is concluded that as the different objectives led to contrasting dynamics and  
714 performance, it is important to actively consider the choice of objective.

715 Overall, this study demonstrates the flexibility of the chosen MPC framework, which  
716 can easily accommodate for additional terms in the objective functions, allowing  
717 WRRF operators to quickly adapt the plant operation to new management objectives  
718 and to face new performance requirements.

719

720

## 721 **Acknowledgements**

722

723 This work is partly funded by the Innovation Fund Denmark (IFD) under File  
724 No. 7038-00097B Peter A. Stenofts industrial PhD study; Stochastic Predictive Con-  
725 trol of Wastewater Treatment Processes and File No. 7038-00097B.

726

727

## 728 **REFERENCES**

729 Ahn, J. H., Kim, S., Park, H., Rahm, B., Pagilla, K., & Chandran, K. (2010). N<sub>2</sub>O  
730 emissions from activated sludge processes, 2008-2009: Results of a national  
731 monitoring survey in the united states. *Environmental Science and Technology*,  
732 44(12), 4505–4511. <https://doi.org/10.1021/es903845y>

733 Aymerich, I., Rieger, L., Sobhani, R., Rosso, D., & Corominas, L. (2015). The  
734 difference between energy consumption and energy cost: Modelling energy tariff  
735 structures for water resource recovery facilities. *Water Research*, 81, 113–123.  
736 <https://doi.org/10.1016/j.watres.2015.04.033>

737 Bartram, D., Shart, M. D., Ebie, Y., Farkas, J., Gueguen, C., Peters, G. M.,  
738 Zanzottera, N. M., Karthik, M., (2019), Chapter 6 – Wastewater treatment and  
739 discharge, refinement to the 2006 IPCC guidelines for National Greenhouse Gas  
740 Inventories, IPCC, Geneva, Switzerland

741 Bellandi, G., Weijers, S., Gori, R., & Nopens, I. (2020). Towards an online mitigation  
742 strategy for N<sub>2</sub>O emissions through principal components analysis and clustering  
743 techniques. *Journal of Environmental Management*, 261.  
744 <https://doi.org/10.1016/j.jenvman.2020.110219>

745 Bernardelli, A., Marsili-Libelli, S., Manzini, A., Stancari, S., Tardini, G., Montanari,  
746 D., Anceschi, G., Gelli, P., Venier, S. (2020). Real-time model predictive control of a  
747 wastewater treatment plant based on machine learning. *Water Science and*  
748 *Technology*, 81(11), 2391–2400. <https://doi.org/10.2166/wst.2020.298>

749 Blum, J.-M., Jensen, M. M., & Smets, B. F. (2018a). Nitrous oxide production in  
750 intermittently aerated Partial Nitritation-Anammox reactor: oxic N<sub>2</sub>O production  
751 dominates and relates with ammonia removal rate. *Chemical Engineering Journal*  
752 (1996. Print), 335, 458–466. <https://doi.org/10.1016/j.cej.2017.10.146>

753 Blum, J.-M., Su, Q., Ma, Y., Valverde Pérez, B., Domingo-Felez, C., Jensen, M. M.,  
754 & Smets, B. F. (2018b). The pH dependency of N-converting enzymatic processes,

755 pathways and microbes: effect on net N<sub>2</sub>O production. *Environmental Microbiology*,  
756 20(5), 1623–1640. <https://doi.org/10.1111/1462-2920.14063>

757 Brok, N.B., Stentoft, P.A., Munk-Nielsen, T., and Madsen, H. (2019). Flexible  
758 control of wastewater aeration for cost-efficient, sustainable treatment. *IFAC-*  
759 *papersonline*, 52(4), 494–499. doi:10.1016/j.ifacol.2019.08.259.

760 Cao, S. Y., (2011) .Mass flow and energy efficiency of municipal wastewater  
761 treatment plants. IWA Publishing.

762 Carstensen, J., Harremoes, P., and Madsen, H. (1995). Statistical identification  
763 of monod-kinetic parameters from on-line measurements. *Water Science and*  
764 *Technology*, 31(2), 125–133.

765 Daelman, M. R. J., van Voorthuizen, E. M., van Dongen, U. G. J. M., Volcke, E. I. P.,  
766 & van Loosdrecht, M. C. M. (2015). Seasonal and diurnal variability of N<sub>2</sub>O  
767 emissions from a full-scale municipal wastewater treatment plant. *Science of the Total*  
768 *Environment*, 536, 1–11. <https://doi.org/10.1016/j.scitotenv.2015.06.122>

769 Danish Ministry of Taxation (2020). Danish Wastewater Taxation Act.  
770 Bekendtgørelse af lov om afgift af spildevand (Spildevandsafgiftloven), LBK nr 478  
771 af 14/04/2020. Danish Ministry of Taxation, Denmark.

772 Delre, A., ten Hoeve, M., & Scheutz, C. (2019). Site-specific carbon footprints of  
773 Scandinavian wastewater treatment plants, using the life cycle assessment approach.  
774 *Journal of Cleaner Production*, 211, 1001–1014.  
775 <https://doi.org/10.1016/j.jclepro.2018.11.200>

776 Domingo Félez, C., & Smets, B. F. (2016). A consilience model to describe N<sub>2</sub>O  
777 production during biological N removal. *Environmental Science: Water Research and*  
778 *Technology*, 2(6), 923–930. <https://doi.org/10.1039/C6EW00179C>

779 Domingo-Félez, C., & Smets, B. F. (2019). Regulation of key N<sub>2</sub>O production  
780 mechanisms during biological water treatment. *Current Opinion in Biotechnology*, 57,  
781 119–126, 119–126. <https://doi.org/10.1016/j.copbio.2019.03.006>

782 Duan, Q., Y., Gupta, V., K., and Sorooshian, S. (1993). Shuffled complex evolution  
783 approach for effective and efficient global minimization. *Journal of Optimization*  
784 *Theory and Applications*, 76(3), 501–521. doi:10.1007/BF00939380.

785 Energinet. (2020). Energisystemet lige nu (English: "Energisystem now"), Ballerup,  
786 Denmark. [https://energinet.dk/energisystem\\_fullscreen](https://energinet.dk/energisystem_fullscreen) [visited 12-09-2020]

787 Escriva-Bou, A., Lund, J. R., & Pulido-Velazquez, M. (2018). Saving Energy From  
788 Urban Water Demand Management. *Water Resources Research*, 54(7), 4265–4276.  
789 <https://doi.org/10.1029/2017WR021448>

790 Foscoliano, C., Del Vigo, S., Mulas, M., & Tronci, S. (2016). Predictive control of an  
791 activated sludge process for long term operation. *Chemical Engineering Journal*, 304,  
792 1031–1044. <https://doi.org/10.1016/j.cej.2016.07.018>

793 Henze, M., Gujer, W., Mino, T., & van Loosdrecht, M. C. M. (2000). *Activated*  
794 *sludge models ASM1, ASM2, ASM2d and ASM3*, Vol. 9, IWA Publishing.

795 Holenda, B., Domokos, E., Redey, A., & Fazakas, J. (2008). Dissolved oxygen  
796 control of the activated sludge wastewater treatment process using model predictive

797 control. Computers and Chemical Engineering, 32(6), 1270–1278.

798 <https://doi.org/10.1016/j.compchemeng.2007.06.008>

799 Isaacs, S., and Thornberg D. 1998. Rule Based Control of a Periodic Activated Sludge  
800 Process. Water Science and Technology 38 (3). doi:10.1016/S0273-1223(98)00468-

801 5.Kirchem, D., Lynch, M., Bertsch, V., & Casey, E. (2018). Market effects of  
802 industrial demand response and flexibility potential from wastewater treatment  
803 facilities. International Conference on the European Energy Market, Eem, 2018-,  
804 8469974. <https://doi.org/10.1109/EEM.2018.8469974>

805 [Jeppsson, U., Pons, M. N., Nopens, I., Alex, J., Copp, J. B., Gernaey, K., ...  
806 Vanrolleghem, P. A. \(2007\). Benchmark simulation model no 2: general protocol and  
807 exploratory case studies. Water Science and Technology, 56\(8\), 67–78.  
808 <https://doi.org/10.2166/wst.2007.604>](#)

809 Kristensen K, Nielsen A, Berg CW, Skaug H, Bell BM (2016). “TMB: Automatic  
810 Differentiation and Laplace Approximation.” Journal of Statistical Software, 70(5), 1–  
811 21. doi: 10.18637/jss.v070.i05.

812 Langergraber, G., Alex, J., Weissenbacher, N., Woerner, D., Ahnert, M., Frehmann,  
813 T., ... Winkler, S. (2008). Generation of diurnal variation for influent data for  
814 dynamic simulation. Water Science and Technology, 57(9), 1483–1486.  
815 <https://doi.org/10.2166/wst.2008.228>

816 Leerbeck, K., Bacher, P., Junker, R. G., Goranović, G., Corradi, O., Ebrahimi, R., ...  
817 Madsen, H. (2020a). Short-term forecasting of CO2 emission intensity in power grids  
818 by machine learning. Applied Energy, 277, 115527.  
819 <https://doi.org/10.1016/j.apenergy.2020.115527>

820 Leerbeck, K., Bacher, P., Junker, R. G., Tveit, A., Corradi, O., & Madsen, H. (2020b).  
821 Control of heat pumps with CO<sub>2</sub> emission intensity forecasts. *Energies*, 13(11), 2851.  
822 <https://doi.org/10.3390/en13112851>

823 Lindstrøm Sørensen, M., Dahl, P., Stentoft, P.A., Munk-Nielsen, T., and Kloppenborg  
824 Møller, J. (2019). Stochastic model predictive control of phosphorus concentration for  
825 smart power, cost-effective municipal wastewater treatment. *Watermatex 2019*,  
826 10th IWA Symposium on Modelling and Integrated Assessment

827 Lisk, B., & Long, H. (2013). Demand management strategies resulting in “zero and  
828 low cost” energy saving opportunities for water and wastewater treatment facilities.  
829 86th Annual Water Environment Federation Technical Exhibition and Conference,  
830 Weftec 2013, 3, 1705–1714. <https://doi.org/10.2175/193864713813673316>

831 Longo, S., d'Antoni, B. M., Bongards, M., Chaparro, A., Cronrath, A., Fatone, F., ...  
832 Hospido, A. (2016). Monitoring and diagnosis of energy consumption in wastewater  
833 treatment plants. A state of the art and proposals for improvement. *Applied Energy*,  
834 179, 1251–1268. <https://doi.org/10.1016/j.apenergy.2016.07.043>

835 Longo, S., Chitnis, M., Mauricio-Iglesias, M., and Hospido, A. (2020). Transient and  
836 persistent energy efficiency in the wastewater sector based on economic  
837 foundations. *Energy Journal*, 41(01).  
838 doi:10.5547/01956574.41.6.slon,10.5547/ISSN0195-6574-EJ

839 Lund, N. S. V., Falk, A. K. V., Borup, M., Madsen, H., & Mikkelsen, P. S. (2018).  
840 Model predictive control of urban drainage systems: A review and perspective  
841 towards smart real-time water management. *Critical Reviews in Environmental*

842 Science and Technology, 48(3), 279–339.

843 <https://doi.org/10.1080/10643389.2018.1455484>

844 Mulas, M., Tronci, S., Corona, F., Haimi, H., Lindell, P., Heinonen, M., ... Baratti, R.

845 (2015). Predictive control of an activated sludge process: An application to the

846 Viikinmaki wastewater treatment plant. *Journal of Process Control*, 35, 89–100.

847 <https://doi.org/10.1016/j.jprocont.2015.08.005>

848 Nielsen, M. K., & Onnerth, T. B. (1995). Improvement of a recirculating plant by

849 introducing star control. *Water Science and Technology*, 31(2), 171–180.

850 [https://doi.org/10.1016/0273-1223\(95\)00190-X](https://doi.org/10.1016/0273-1223(95)00190-X)

851 Nordpool, (2020), Market Data, Nordpool group, Oslo, Norway, Available at:

852 <https://www.nordpoolgroup.com/Market-data1/#/nordic/table> [visited 12-09-2020]

853 Olsson, G. (2015). “Water and Energy: Threats and Opportunities - Second Edition”.

854 und. In: *Water Intelligence Online* 14. ISSN: 14761777. DOI:10.2166/9781780406947

855 Porro, J., Bellandi, G., Rodriguez-Roda, I., Deeke, A., Weijers, S., Vanrolleghem, P.,

856 ... Nopens, I. (2017). Developing an artificial intelligence-based WRRF nitrous oxide

857 mitigation road map: The Eindhoven N<sub>2</sub>O mitigation case study. *Water Environment*

858 Federation Technical Exhibition and Conference 2017, Weftec 2017, 3, 1568–1580.

859 REN21. 2020. *Renewables 2020 Global Status Report*, Paris: REN21 Secretariat,

860 ISBN 978-3-948393-00-7

861 Stentoft, P.A., Munk-Nielsen, T., Mikkelsen, P.S., and Madsen, H. (2017). A

862 stochastic method to manage delay and missing values for in-situ sensors in an alter-

863 nating activated sludge process. Proceedings of the 12<sup>th</sup> Iwa Specialized Conference  
864 on Instrumentation, Control and Automation.

865 Stentoft, P.A., Guericke, D., Munk-Nielsen, T., Mikkelsen, P.S., Madsen, H., Vezzaro,  
866 L., and Møller, J.K. (2019a). Model predictive control of stochastic wastewater treat-  
867 ment process for smart power, cost-effective aeration. Proceedings of Dycops  
868 2019.

869 Stentoft, P.A., Munk-Nielsen, T., Vezzaro, L., Madsen, H., Mikkelsen, P.S., and  
870 Møller, J.K. (2019b). Towards model predictive control: online predictions of  
871 ammonium and nitrate removal by using a stochastic ASM. Water Science and  
872 Technology, 79(1), 51–62. doi:10.2166/wst.2018.527

873 Stentoft, P. A., Vezzaro, L., Mikkelsen, P. S., Grum, M., Munk-Nielsen, T., Tychsen,  
874 P., ... Halvgaard, R. (2020a). Integrated model predictive control of water resource  
875 recovery facilities and sewer systems in a smart grid: example of full-scale  
876 implementation in Kolding. Water Science and Technology : a Journal of the  
877 International Association on Water Pollution Research, 81(8), 1766–1777.  
878 <https://doi.org/10.2166/wst.2020.266>

879 Tchobanoglous, G.; Burton, F.L; Stensel, H.D., 2004. Wastewater engineering  
880 treatment and reuse, 4th Edition. McGraw-Hill: New York.

881 Vasilaki, V., Volcke, E. I. P., Nandi, A. K., van Loosdrecht, M. C. M., & Katsou, E.  
882 (2018). Relating N<sub>2</sub>O emissions during biological nitrogen removal with operating  
883 conditions using multivariate statistical techniques. Water Research, 140, 387–402.  
884 <https://doi.org/10.1016/j.watres.2018.04.052>



885 Yamanaka, O., Obara, T., & Yamamoto, K. (2006). Total cost minimization control  
886 scheme for biological wastewater treatment process and its evaluation based on the  
887 COST benchmark process. *Water Science and Technology*, 53(4-5), 203–214.  
888 <https://doi.org/10.2166/wst.2006.125>

889 Yuan, Z., Olsson, G., Cardell-Oliver, R., van Schagen, K., Marchi, A., Deletic, A.,  
890 Urich, C., Rauch, W., Liu, Y., and Jiang, G. (2019). Sweating the assets the role of  
891 instrumentation, control and automation in urban water systems. *Water Research*,  
892 155, 381–402. doi:10.1016/j.watres.2019.02.034

893

## TABLES AND FIGURES

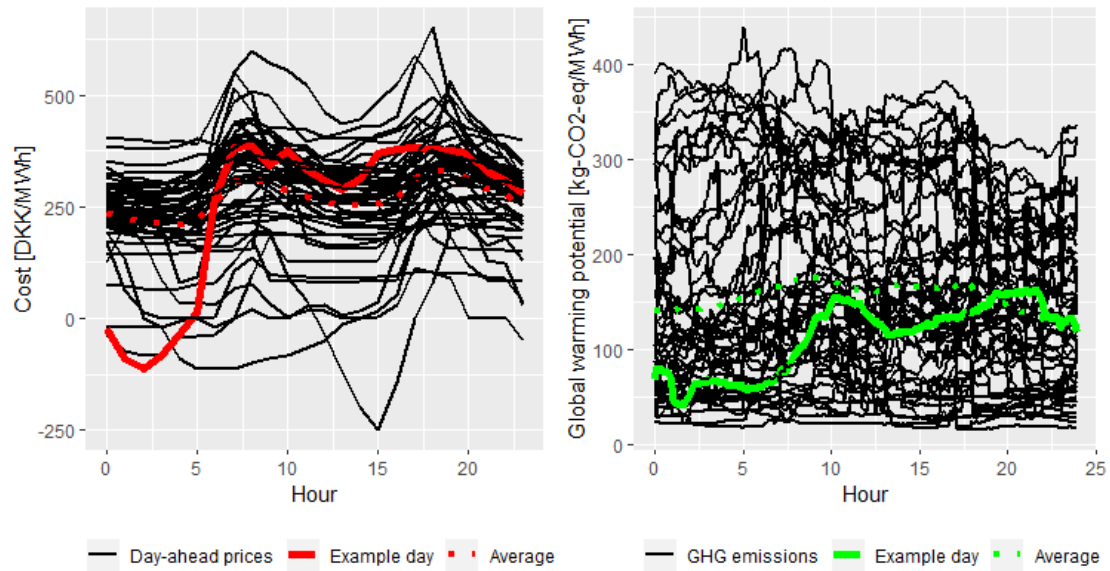


**Figure 1** Electricity prices for the Denmark West market (Nordpool, 2020) and (b) GHG emissions from electricity production (Energinet, 2020) for the Nordic electricity market, for the 51 days in the period from 2019/01/14 to 2020/02/18. The example day (2019/01/14) is highlighted.

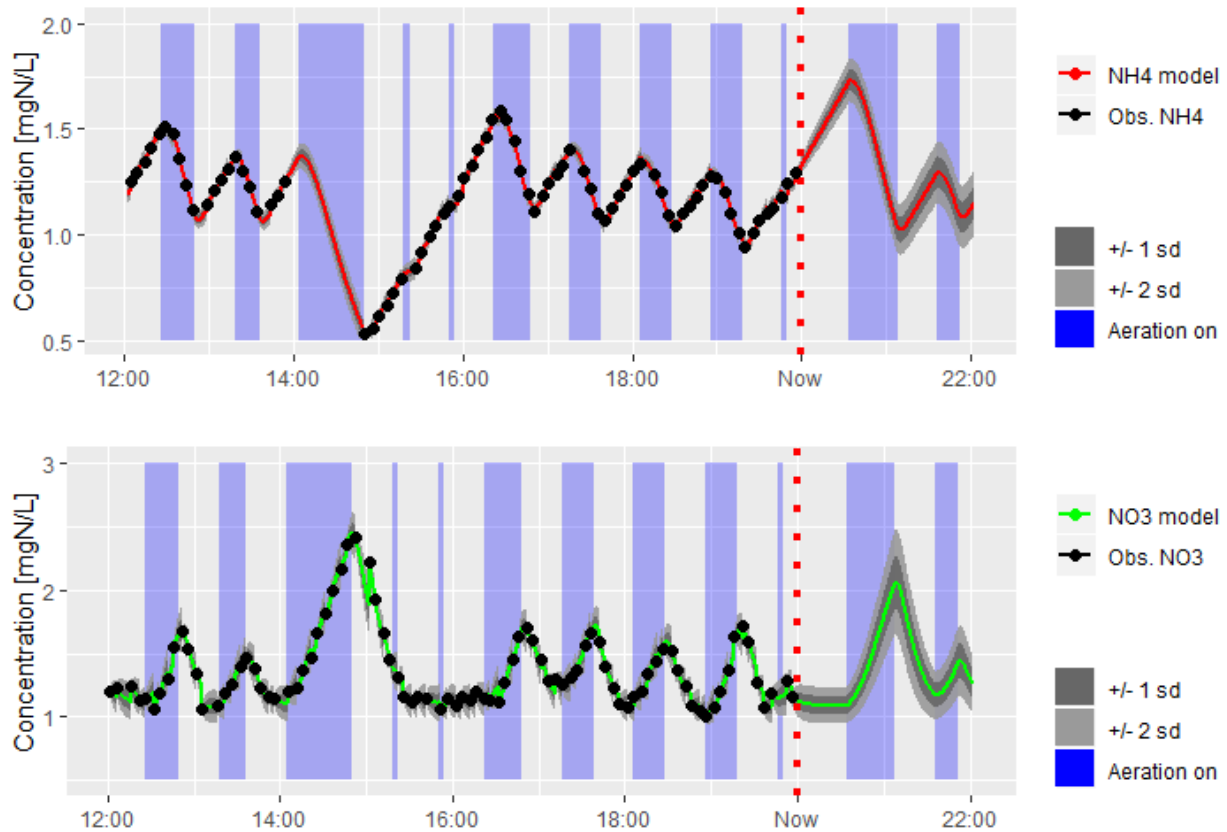


**Figure 2** Model fitted to ammonium and nitrate data from Nørre Snede WRRF for the example day (2019/01/14), including a prediction 2 hours ahead from 20:00 (“now”). The estimated parameters related to this fit are shown in Table 1. The grey areas highlight the uncertainty of the model predictions. Note that uncertainty increases as prediction horizon increases. This is to emphasize that the “known” observations are further back, and hence it is more difficult to predict accurately.

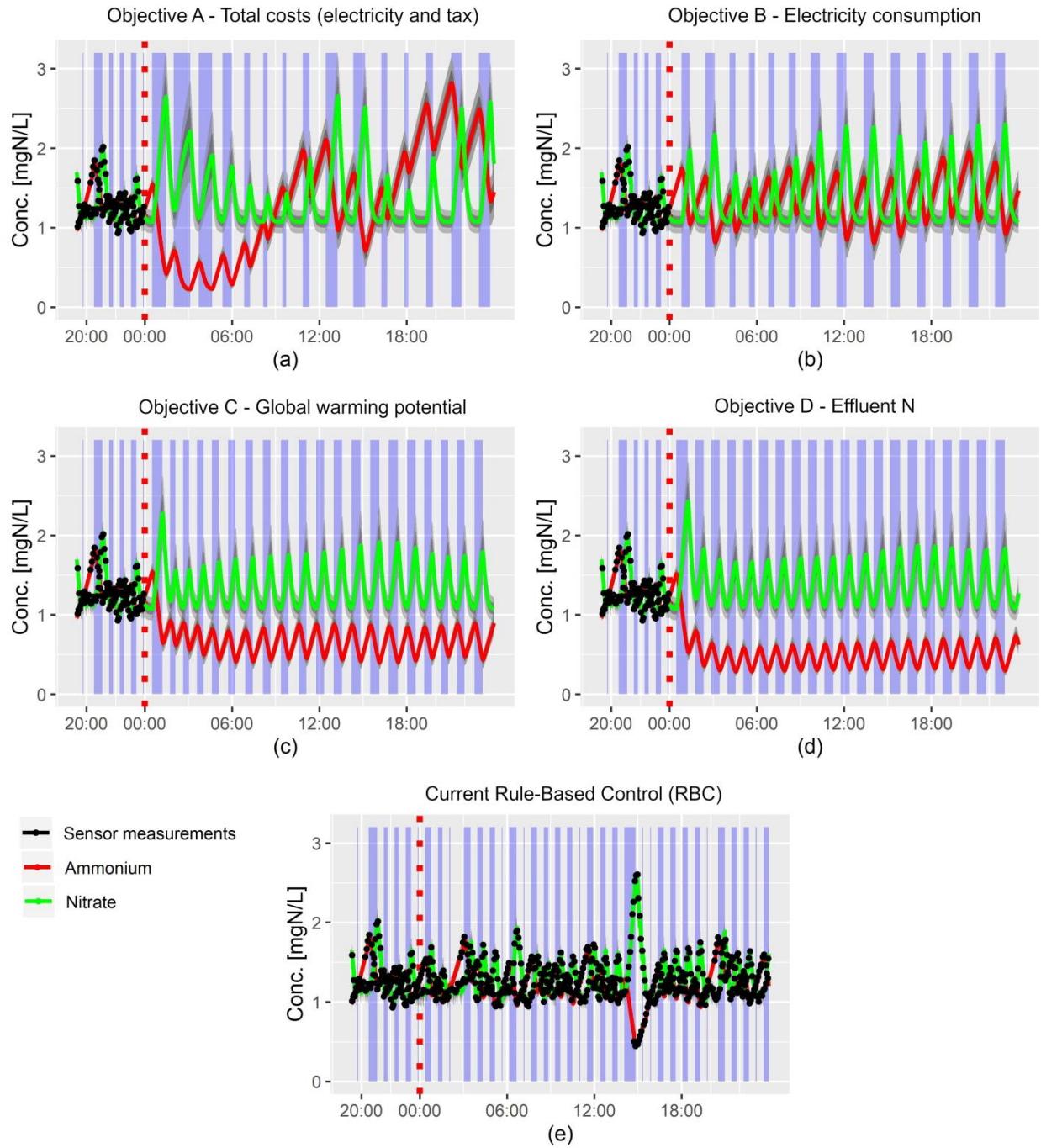


**Figure 3.** Ammonium and nitrate concentration and aeration controls obtained with different control scenarios 24 hours ahead (example day - starting from 2019/01/14 00:00): (a) optimization of total operational costs, (b) optimization of electricity consumption, (c), optimization of global warming potential, (d) optimization of effluent total-N, and (e) current rule-based control. Aeration phases are shown by the different background colors: on (blue) and off (grey).

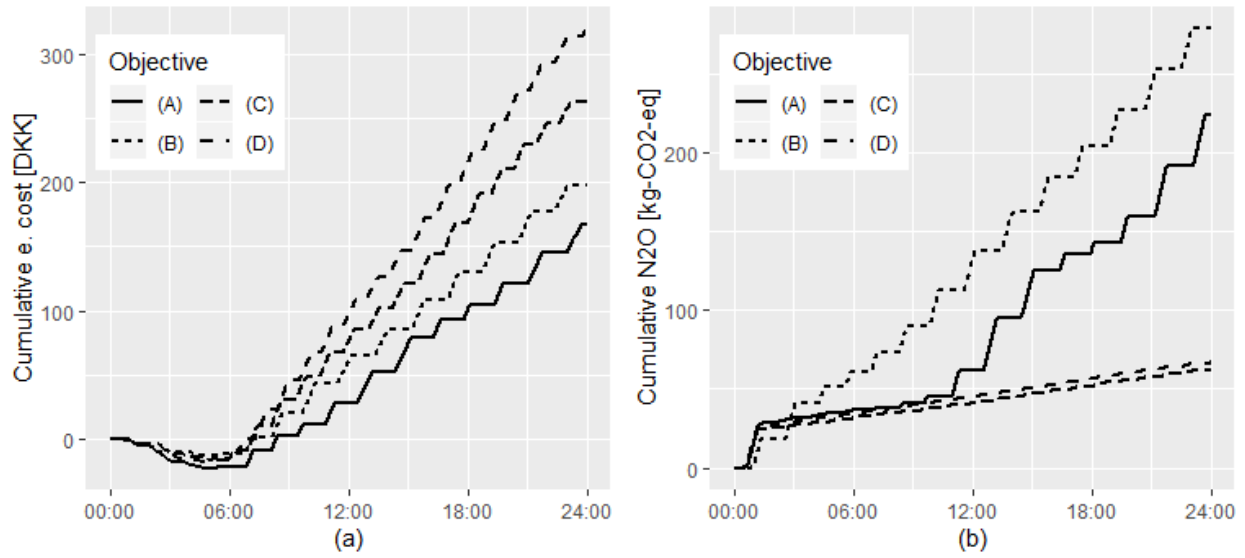


**Figure 4** (a) Cumulative electricity costs and (b) N<sub>2</sub>O emissions from process for the four control scenarios over the example day.

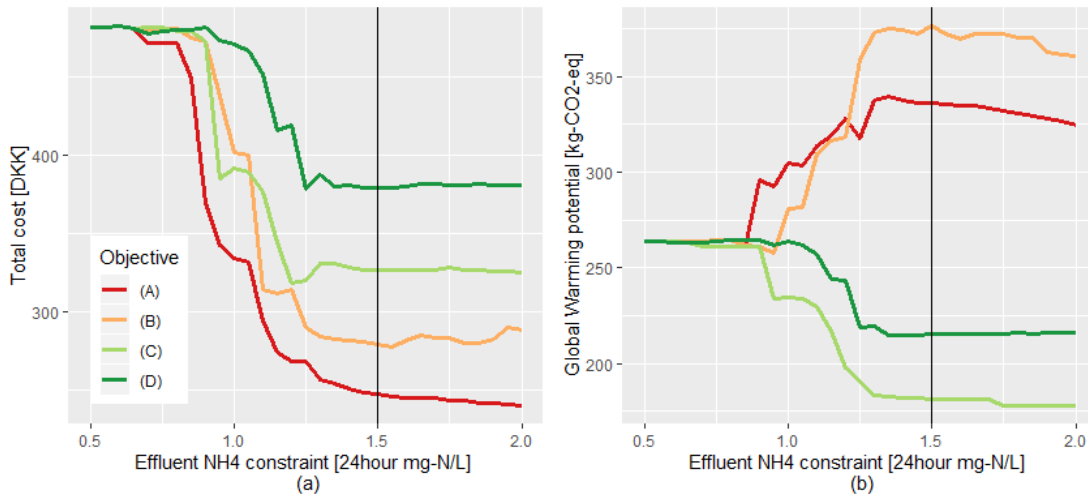


**Figure 5** Effect of different constraints on effluent NH<sub>4</sub> concentration on (a) total costs and (b) GWP for different control scenarios on the example day. The black line shows the limit used for the results shown in Figure 2 and 3.

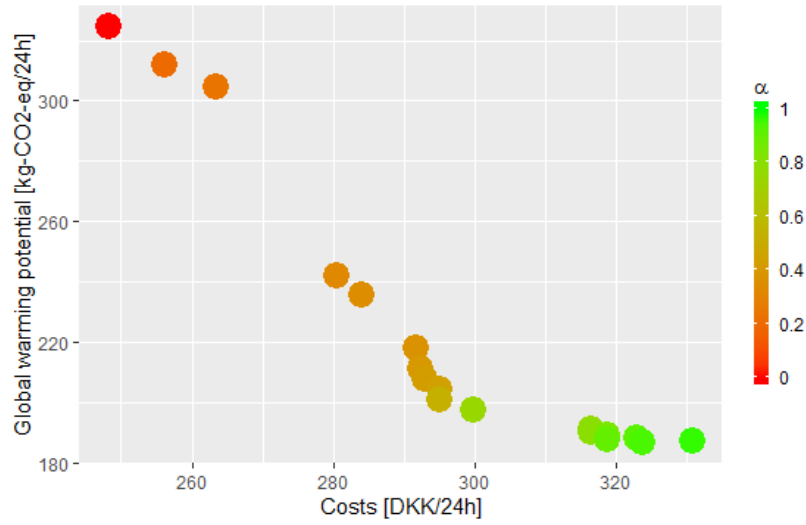


**Figure 6** Trade-off between total costs and global warming potential using a combined objective function (eq. 18) for the different values of  $\alpha$  ( $\alpha=0$  corresponds to cost prioritization only,  $\alpha=1$  corresponds to GWP prioritization only).

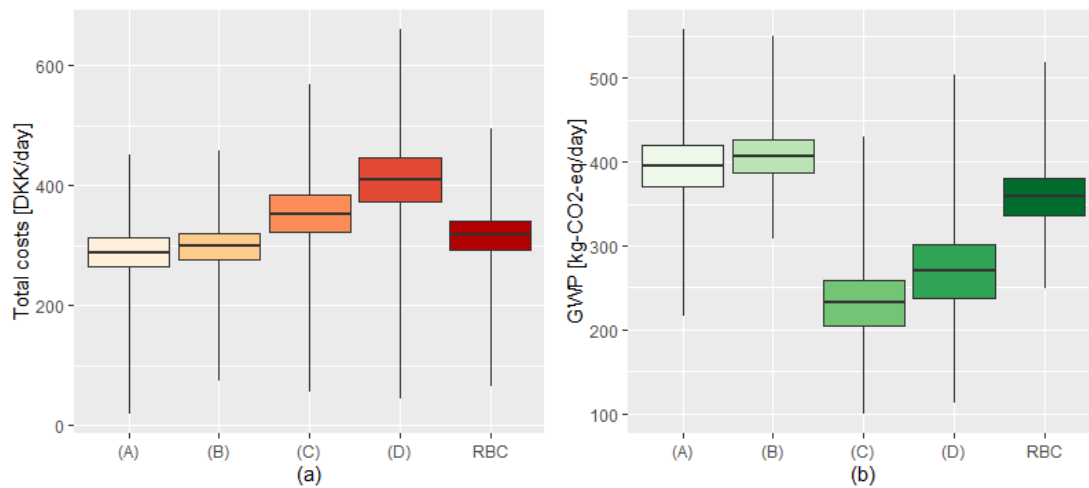


**Figure 7** Boxplots showing (a) total costs and (b) global warming potential obtained for the 51 simulated days (shown in Figure 1) by using the four control scenarios (A-D) and the current rule-based control (RBC). The boxplots show max/min (whiskers),  $\pm 2$  standard deviations (coloured space) and the mean (horizontal black lines).

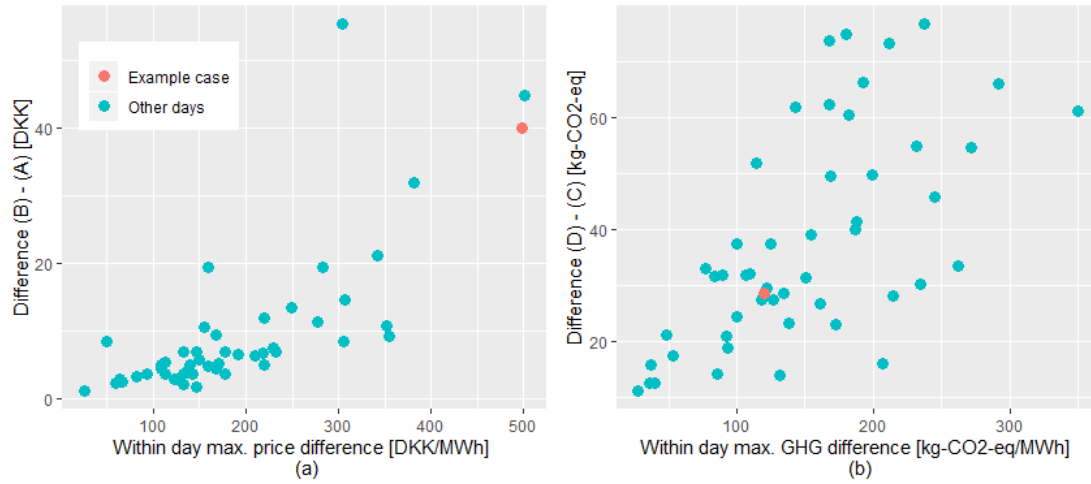


**Figure 8** (a) Difference in total daily cost between Objective A and B as a function of inter-diurnal price variations (max – min) (b) Difference in GWP between objectives C and D as a function of inter-diurnal variations in GHG emission from electricity production (min-max). Results are shown for the 51 simulated days, while the example day is marked in red.

**Table 1** List of parameters and state variables of the data-driven Activated Sludge Model for nitrogen removal. The last column shows the estimate obtained using 24 hours of ammonium and nitrate measurements from Nørre Snede WRRF on the example day (2019/01/14).

<i>Parameter</i>	<i>Description</i>	<i>Unit</i>	<i>Estimate for example day</i>
$\kappa_1$	Rate for incoming WW	[]	0.27
$\kappa_2$	Rate for change in incoming NH <sub>4</sub>	[]	0.62
$r_{Ni}$	Nitrification rate	mgNL <sup>-1</sup> min <sup>-1</sup>	0.05
$r_{Dni}$	Denitrification rate	mgNL <sup>-1</sup> min <sup>-1</sup>	0.11
$m_{NH}$	minimum observable NH <sub>4</sub> conc.	mgNL <sup>-1</sup>	0.14
$m_{NO}$	minimum observable NO <sub>3</sub> conc.	mgNL <sup>-1</sup>	0.92
$K_{NH}$	Monod inspired affinity coefficient for NH <sub>4</sub> .	min	1.81
$K_{NO}$	Monod inspired affinity coefficient for NO <sub>3</sub> .	min	1.97
$\mu_{in,NH}$	Mean incoming NH <sub>4</sub> conc.	mgNL <sup>-1</sup>	67.9
$\mu_{in,NO}$	Mean incoming NO <sub>3</sub> conc.	mgNL <sup>-1</sup>	0.01 (fixed)
$\sigma_1$	Model noise parameter related to $S_{NH}$	mgNL <sup>-1</sup>	0.02
$\sigma_2$	Model noise parameter related to $S_{NO}$	mgNL <sup>-1</sup>	0.04
$\sigma_3$	Model noise parameter related to $S_{\mu}$	mgNL <sup>-1</sup>	0.06
<b>Aeration term, <math>O_j</math> (eq. 5)</b>			
$\kappa_3$	Rate for skewness in the oxygen signal	[]	3.00
$\kappa_4$	Rate for increase in oxygen after start	[]	0.19
$D_j$	The "delay" of observations	min	1.89
$\tau_{on,i}$	The switch aeration "on" times	min	Input
$\tau_{off,i}$	The switch aeration "off" times	min	Input
<b>State variables, <math>S_x</math></b>			
$S_{NH}$	Ammonium concentration in tank	mgNL <sup>-1</sup>	variable
$S_{NO}$	Nitrate concentration in tank	mgNL <sup>-1</sup>	variable
$S_{\mu}$	Inlet flux of incoming ammonium	mgNL <sup>-1</sup>	variable



**Table 2** Parameter of the objective functions used in the optimization of the Nørre Snede WRRF.

Parameter	Description	Value
$E_C$	Equipment consumption [MW]	0.1
$T_N$	Effluent tax [DKK/kg-N]	30.0
$L_{NH}$	Ammonium limit [mg-N/L/24h]	1.5
$L_N$	Total-N limit [mg-N/L/24h]	2.9
$\tau_{min,on}$	Min duration of aeration phase [min]	10
$\tau_{max,on}$	Max duration of aeration phase [min]	80
$\tau_{min,off}$	Min duration of no-aeration phase [min]	30
$\tau_{max,off}$	Max duration of no-aeration phase [min]	80
$C_{N_2O,CO_2}$	N <sub>2</sub> O GWP-contribution [kg-CO <sub>2</sub> -eq/kg-N <sub>2</sub> O]	298
$E_{f,N_2O}$	N <sub>2</sub> O produced due to effluent N	0.005
$r_{N_2O,low}$	N <sub>2</sub> O emission $r_{NH}<5\text{mg TAN}/(\text{g-VSS}\cdot\text{h})$ []	0.01
$r_{N_2O,high}$	N <sub>2</sub> O emission $r_{NH}>5\text{mg TAN}/(\text{g-VSS}\cdot\text{h})$ []	0.09
Z	Large number for the soft constraints	10000
VSS	Volatile suspended solids [g/L]	3

**Table 3.** Performance indicators from application of the four different management objectives (A-D) and the current control (RBC) on the example day (Figure 1). The indicator targeting the goal of the objective functions is highlighted in bold and a frame. In addition the lowest value for each performance indicator is highlighted in bold. Effluent concentrations are estimated as average over 24 hours. Average electricity price/GWP are the obtained values over the 24 hours with variable inputs. N<sub>2</sub>O emissions cover both the direct and indirect N<sub>2</sub>O.

Performance indicator	A	B	C	D	RBC*
Effluent NH <sub>4</sub> [mgN/L]	1.33	1.36	0.69	<b>0.52</b>	1.25
Effluent NO <sub>3</sub> [mgN/L]	1.41	1.36	1.35	1.39	<b>1.30</b>
Effluent total-N [mgN/L]	2.74	2.72	2.04	<b>1.91</b>	2.55
Total Cost [DKK]	<b>247.7</b>	279.4	324.2	377.2	307.7
Electricity cost [DKK]	<b>165.2</b>	197.8	263.0	319.7	231.2
Effluent tax [DKK]	82.4	81.6	61.2	<b>57.5</b>	76.5
Relative Aeration [% "on"-time]	39.5	<b>33.3</b>	44.6	53.7	37.1
Average price of consumed electricity [DKK/MWh]	<b>174.2</b>	247.5	245.7	248.0	259.8
Average GWP of consumed electricity [kg-CO <sub>2</sub> -eq/MWh]	<b>102.7</b>	114.0	113.1	112.6	115.6
GWP, N <sub>2</sub> O contribution[kg-CO <sub>2</sub> -eq]	227.9	282.4	<b>64.7</b>	69.2	219.6
GWP from electricity production [kg-CO <sub>2</sub> -eq]	96.8	<b>91.1</b>	121.0	145.2	102.9
GWP, total [kg-CO <sub>2</sub> -eq]	324.6	373.5	<b>185.7</b>	214.4	322.5